Int. J. Electrochem. Sci., 7 **(2012)** 9202 - 9212

International Journal of
ELECTROCHEMICAL
SCIENCE
www.electrochemsci.org

Evaluation of Simulated Atmospheric Corrosion of Q235 Steel by Wavelet Packet Image Analysis

Zhi-ming Gao[*] *Xia-bing Han, Li-hua Dang, Ying Wang, Hui-chao Bi*

School of Material Sciences and Engineering, Tianjin University, Tianjin 300072,P.R. China
[*]E-mail: gaozhiming@tju.edu.cn

Received: 14 August 2012 / *Accepted:* 11 September 2012 / *Published:* 1 October 2012

The corrosion morphology of Q235 steel in simulated atmospheric environment was obtained using the established image acquisition system which can be used in the field. In order to obtain the detailed information of the images, wavelet packet decomposition–based image analysis method was applied to decompose the improved images and energies of sub-images (according to the Shannon entropy standard to choose the optimal sub-images with high regularity) were extracted as characteristic information. The results showed that it is the change of the energies of sub-images that can make a qualitative analysis of the corrosion degree of Q235 steel specimens. The relationship between the feature value and corrosion weight loss of samples was evaluated by regression analysis. By using the equation given by the regression analysis, the corrosion degree of Q235 steel specimens can be quantitatively analyzed. The proposed method can be used to predict the atmospheric corrosion of steel.

Keywords: Atmospheric corrosion; Corrosion morphology; Wavelet Packet Decomposition; Image analysis; Corrosion prediction

1. INTRODUCTION

Atmospheric corrosion is a process of practical importance as it degrades the structures, devices and products exposed to atmosphere [1]. The atmospheric corrosion behaviors and mechanisms of metal materials have been studied around the world for many years [2-5]. Corrosion rates of metals are often determined from the weight changes of samples after removal of the corrosion products [6-8]. However, weight change measurements are not appropriate to evaluate local corrosion and the initial corrosion [9].

The corrosion performance of metal material can be characterized by corrosion rate as well as corrosion morphology analysis. Image analysis is an appropriate tool to characterize qualitatively and

quantitatively the early stage of the mechanism of damage by corrosion [10-12]. The corrosion morphology image acquisition system which can be used in the laboratory was established by Shizhe Song et al. [13-15], their research object was field exposured high strength aluminium alloys and periodic rain accelerated corrosion of aeronautical aluminium alloys[16-18]. Shizhe Song et al. have made a preliminary study of the application of image analysis use in corrosion science.

The first formants in conjunction with the Shannon entropy of wavelet packet (WP) upon level four features extraction method was developed by Khaled Daqrouq [19] for speech based text-independent speaker identification. Deng Wang et al. [20] put forward that representation original electroencephalo-graph signals by wavelet packet coefficients and feature extraction using the best basis-based wavelet packet entropy method. Xiangyang Luo et al. [21] present a new blind image steganalysis method based on wavelet package decomposition (WPD), which can detect the stego images with comparatively high accuracy, make a research on the application of WP use in images analysis. The methods of wavelet packets analysis have been successfully used for image analysis [19-21].

In this paper, image analysis method based on WPD(decomposes both details and approximations) was used to study the early stage corrosion morphology of Q235 steel in oder to overcome the problem that wavelet analysis only performing the decomposition process on approximations. The corrosion morphology was obtained using the established image acquisition system that can be used in the field. This method was applied to decompose the improved images and obtain the detailed information of the images. According to the Shannon entropy standard to choose the optimal sub-images with high regularity, the energies of the optimal sub-images were extracted as characteristic information. Based on the variation of image feature values, the corrosion degree of Q235 steel specimens was quantitatively and quantitatively analyzed.

2. EXPERIMENTAL

2.1 Sample preparation

The chemical composition (in wt. %) of Q235 steel samples (50mm×10mm×2.5mm) are listed as followed: C 0.12-0.20，Mn 0.30-0.70，Si ≤0.3，P≤0.045，S≤0.045， the remaining is Fe. Four parallel samples were tested for each test term: three for weight loss measurement and one for corrosion morphology analysis. The salt spray corrosion test chamber of MNFS-1 was used to simulate the offshore atmospheric environment. The spray solution contains 0.1mol/L NaCl (The offshore atmospheric contains many sea salt particles and the main component of those salt particles is sodium chloride). Setting simulated environment temperature as 30 ℃, relative humidity as 70%.

2.2 Corrosion Image acquisition

Using the VHX-500FE digital video-microscope system (KEYENCE Co. Ltd.) with 20-200× lens that offer a resolution of 1600×1200dpi (dots per inch). This system have a function of real-time depth synthesis, the viewing distance is about 25.5 mm, the format of the output image is RGB UXGA.

The corrosion morphology images of Q235 steel samples were acquired （in the 30×lens） before the corrosion products were removed. The typical corrosion morphology images are shown in Fig.1. Fig.1(a), (b), (c), (d), (e)and(f) indicate the corrosion morphology images of Q235 steel specimens exposed to atmospheric environment for28d, 44d, 52d, 63d, 74d and 81d, respectively.

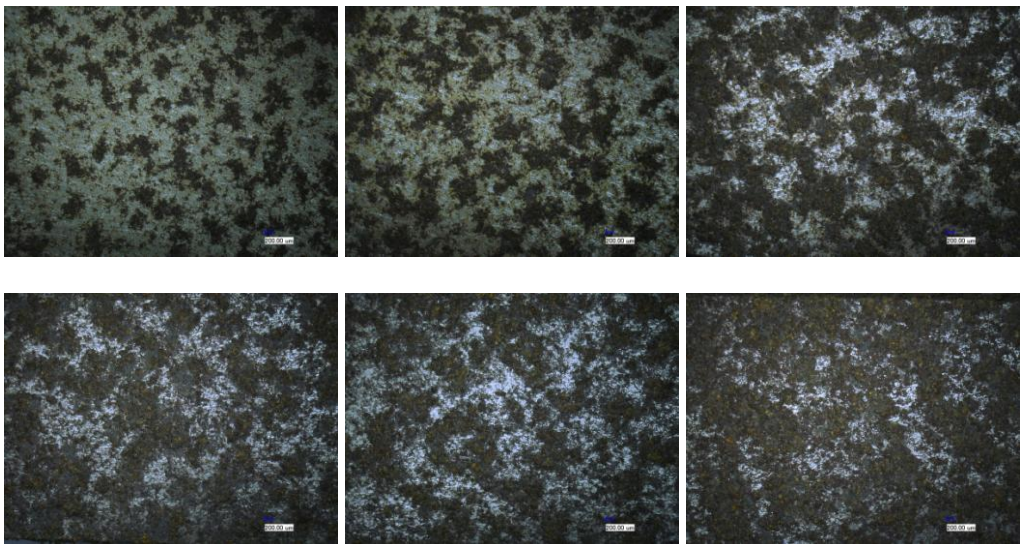

Figure 1. Corrosion morphology of Q235 steel samples (a)28 d; (b)44 d; (c)52 d; (d)63 d; (e)74 d; (f)81 d;

3. THE IMAGE ANALYSIS METHOD OF SIMULATED ATMOSPHERIC CORROSION SPECIMENS

3.1 Image pre-processing

The in situ corrosion morphology images of Q235 steel samples were acquired before the corrosion products were removed. Corrosion rate is measured by weight changes after corrosion product removal. In order to eliminate the impact of fixed holes and marginal area of specimens, the image procession areas of the coupons should be selected. In this paper, the image processing areas (118.4 mm×84.6 mm) in the centre of the Q235 steel specimens was selected. This method has been proved to be an effective way to analyze the samples with irregular shape with limited influence [16].

The corrosion morphology images of Q235 steel samples (a part area of each sample was cut for the surface analysis) were converted to gray images uniformly. Images acquired through modern devices may be contaminated by a variety of noise sources. By noise we refer to stochastic variations as opposed to deterministic distortions such as lack of focus[18]. In the present work, the median filter method and fuzzy enhancement method were applied to make the corrosion morphology features clear.

3.2 Corrosion image analysis based on wavelet packet Decomposition

Wavelet packets can be viewed as a generalization of the structure of the wavelet decomposition to a full decomposition. An image can be considered as two-dimensional signal. In the following, the wavelet transform defined as the inner product of a signal$\varphi(t)$with the mother wavelet $\psi(t)$ [22]:

$$\psi_{a,b}(t) = \psi(\frac{t-b}{a}) \quad (1)$$

$$W_{\psi}\phi(a,b) = \frac{1}{\sqrt{a}}\int_{-\infty}^{+\infty}\phi(t)\times z(\frac{t-b}{a})dt \quad (2)$$

where a and b are the scale and shift parameters, respectively.

The wavelet packet transform generates the full decomposition tree, Fig. 2 gives the comparison of a two-level wavelet packet decomposition[23-24]. A low-pass and high-pass filter is repeatedly used to yield two sequences to capture different frequency sub-band features of the original signal [22]. The two wavelet orthogonal bases generated to form a previous node are defined as

$$\psi_{j+1}^{2p}(k) = \sum_{n=-\infty}^{\infty} h[n]\psi_j^p(k-2/n) \quad (3)$$

$$\psi_{j+1}^{2p}(k) = \sum_{n=-\infty}^{\infty} g[n]\psi_j^p(k-2/n) \quad (4)$$

where h[n] and g[n] denote the low-pass and high-pass filters, respectively. In Eqs. (3) and (4), ψ[n]is the wavelet function. Parameters j and p are the number of decomposition levels and nodes of the previous node, respectively [22]. Because WPD decomposes both details and approximations instead of only performing the decomposition process on approximations, it holds the important information located in higher frequency components than WT in certain applications[20]. The WPD can provide a more precise frequency resolution than WT.

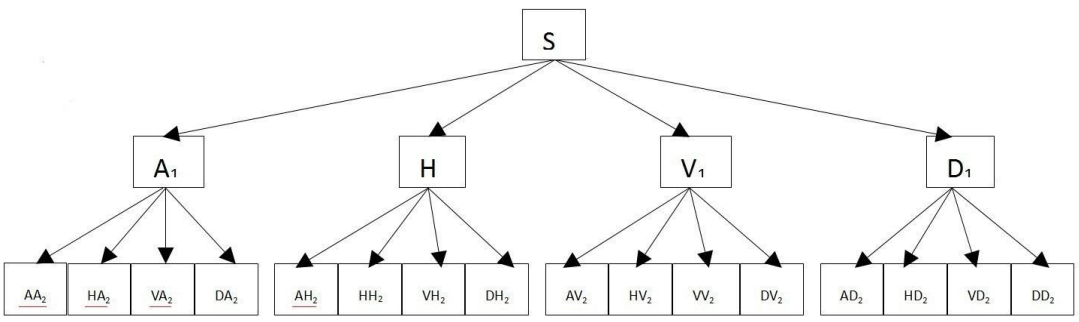

Figure 2. Structure of two-level wavelet packet decomposition

3.2.1 Sub-image selection

The improved images were decomposed by wavelet package decomposition at depth k, with Haar wavelet. Different image characteristics can be analysed by different wavelets, the characteristic information extracted was also different. However, most experiments show that the selection of wavelet only have a little influence on the analysis results[25].

Entropy is a common concept in many fields, mainly in signal processing[26]. Entropy is commonly used in image processing, an image can be considered as two-dimensional signal; it posses information about the concentration of the image[19]. The entropy 'E' must be an additive information cost function such that E(0) = 0 and

$$E = \sum_i E(s_i) \tag{5}$$

where s is the signal and si are the WPT coefficients. E can be as a signal regularity metrics as long as satisfying the conditions mentioned above. Shannon entropy is used in most time [20].

After the decomposition of the improved images, every sub-images contained different information of a special scale and orientation were got, Shannon entropy for all 22knodes at depth k for wavelet packet were calculated using the following equation [26]:

$$\begin{aligned} E1(s_i) &= s_i^2 \log(s_i^2) \\ E1(s) &= -\sum_i s_i^2 \log(s_i^2) \end{aligned} \tag{6}$$

Once the two-level WPD was applied, 16 images were obtained. To find out the regularity of detail coefficients and observe the Shannon entropy values of all 16 nodes at depth 2. According to the Shannon entropy standard (the smaller the entropy, the higher regularity of the information) the optimal sub-images will be selected [26].

3.2.2 Sub-image feature extraction

The improved images were decomposed by wavelet packet. The low-frequency and high-frequency coefficient of sub-image in horizontal, vertical, and diagonally orientation, was got respectively. The size of the improved image is m×n. The feature is calculated as follows[26]:

Energy feature of improved image are as follow：

$$E_{en} = \sum_{i=0,\, j=0}^{i=m,\, j=n} (C^2) \tag{7}$$

Energy feature of sub-image of h (h means different sub-images at the same transformation depth)：

$$E_{wp-h} = [100 \times \sum_{i=0, j=0}^{i=m, j=n} (C_h^2)] / E_{en} \quad (8)$$

Where Ch (h=1,2,…16)is coefficient matrix of sub-image, C is the coefficient matrix of the improved images before decomposed.

In the present work, the energy Ewp of every sub-image was selected as the feature of the corrosion morphology. EHA2, EVA2 and EAH2 denote the energy of sub-image in HA2, VA2and AH2 orientation, respectively. The number of sub-images is defined as "the sub-images orientation of second level+ the sub-images orientation of first level+ the decomposition level".

4. Results and Discussion

4.1 The optimal sub-images of Q235 steel selection

Table 1. Sub-image entropy of Q235 steel corrosion morphological image

Entropy	Sample					
	28d	44d	52d	63d	74d	81d
AA_2	-1.0669	-1.0588	-1.134	-1.1751	-1.0107	-1.1375
HA_2	-0.0016	-0.002	-0.0031	-0.0037	-0.0039	-0.0049
VA_2	-0.0014	-0.0016	-0.0025	-0.0029	-0.0033	-0.004
DA_2	-0.0002	-0.0002	-0.0003	-0.0004	-0.0005	-0.0006
AH_2	-0.0002	-0.0003	-0.0005	-0.0006	-0.0006	-0.0008
HH_2	-0.0002	-0.0002	-0.0003	-0.0004	-0.0004	-0.0005
VH_2	0	0	-0.0001	-0.0001	-0.0001	-0.0001
DH_2	0	0	-0.0001	-0.0001	-0.0001	-0.0001
AV_2	-0.0002	-0.0003	-0.0004	-0.0005	-0.0005	-0.0006
HV_2	0	0	-0.0001	-0.0001	-0.0001	-0.0001
VV_2	-0.0001	-0.0001	-0.0002	-0.0002	-0.0003	-0.0004
DV_2	0	0	-0.0001	-0.0001	-0.0001	-0.0001
AD_2	0	0	0	0	0	0
HD_2	0	0	0	0	0	0
VD_2	0	0	0	0	0	0
DD_2	0	0	0	0	0	0

Legend: The order of magnitude of the data in Table1 is e^{+11}.

Specimens of 16 sub-images in different orientation was obtained after the improved images were decomposed by wavelet packet at depth 2. Shannon entropy for all 16 nodes were calculated at depth 2 with wavelet packet method using equation (6), the results are shown in Table 1.

It is showed that the sub-image entropy in AA2, VA2, HA2 and AH2 orientation is lower than others. In order to study the detailed of the corrosion morphology, three high-frequency sub-images was selected to represent the feature of Q235 steel corrosion morphology.

4.2 Estimate corrosion degree based on image feature

4.2.1 Qualitatively analysis

The sub-image energies of Q235 steel specimens exposed to simulated atmospheric environment are calculated by Eq. (5) and (6). The results are shown in Table. 2. The sub-image energies distribution in different exposure time is shown in Figs.3 and 4.

Table 2. Sub-image energy of Q235 steel corrosion morphological image

Sample No.	Feature Values		
	E_{HA2}	E_{VA2}	E_{AH2}
28d	0.4898	0.4174	0.0964
44d	0.5766	0.4684	0.1128
52d	0.7731	0.632	0.154
63d	0.8999	0.7031	0.175
74d	0.9908	0.8426	0.1906
81d	1.1076	0.9318	0.2157

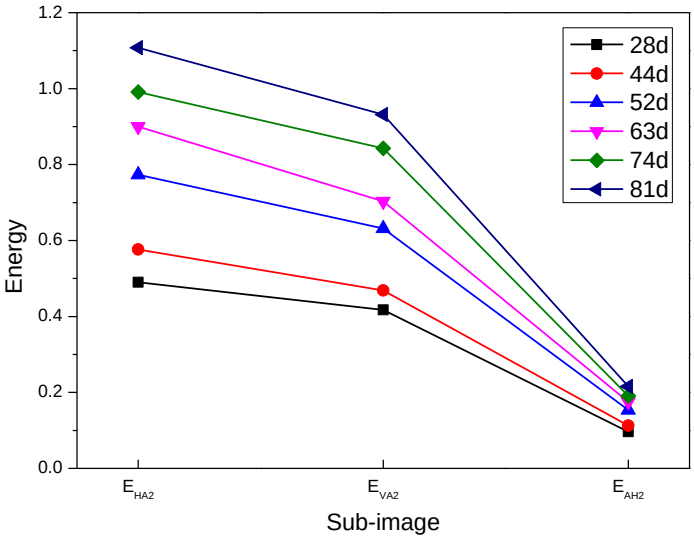

Figure 3. Sub-image energy distribution with different exposure time

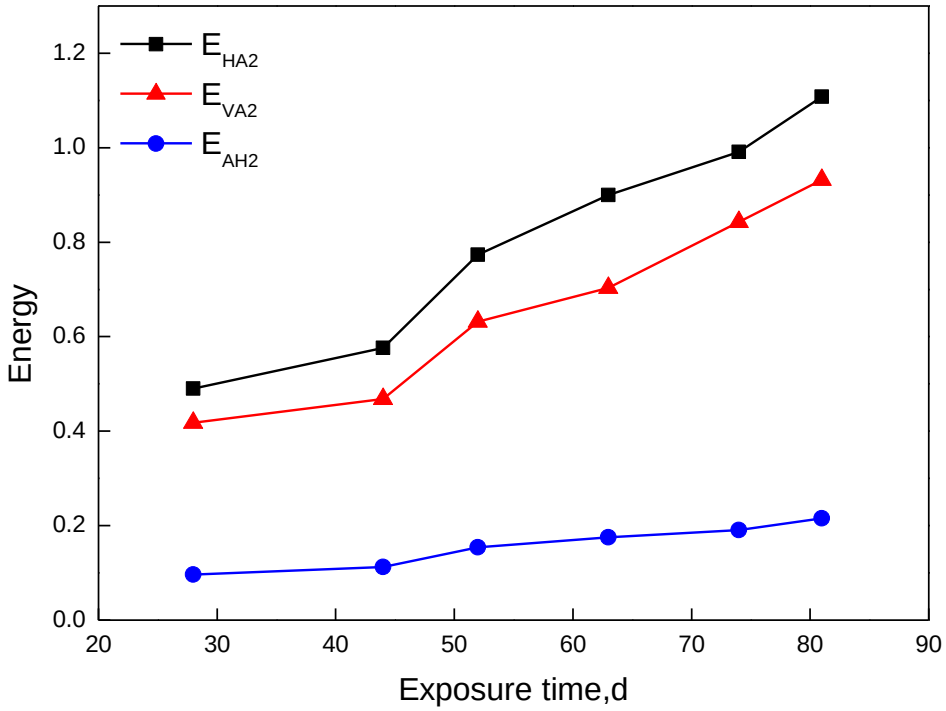

Figure 4. The relationship between Sub-image energy and exposure time

From Fig.3 and 4, It can be easily found that with the increase of the exposure time the energy of sub-image increased. In other words, the sample with shorter exposure time its sub-image has a smaller energy. Results showed that the corrosion degree of Q235 steel specimens was correlated well with the change of the energies of sub-images. The conclusion was basically identical with the result based on the corrosion weight loss.

4.2.2 Quantitatively analysis

The feature value of corrosion morphology images S is calculated as follow:

$$S = E_{HA_2} + E_{VA_2} + E_{AH_2} \quad (9)$$

Fig. 5 gives the fitting result of the feature value S versus corrosion weight loss W. The equation of the curve is given in Eq. (8).

$$W=13.64e^{0.527S} \quad (R=92.4\%) \quad (10)$$

Table 3. Feature values of corrosion morphology images *S* and corrosion weight loss *W*

Sample No.	*W* (g/m^2)	*S*
28d	19.6078	1.0036
44d	26.4314	1.1578
52d	33.7255	1.5591
63d	35.8431	1.778
74d	39.1373	2.024
81d	43.9216	2.2551

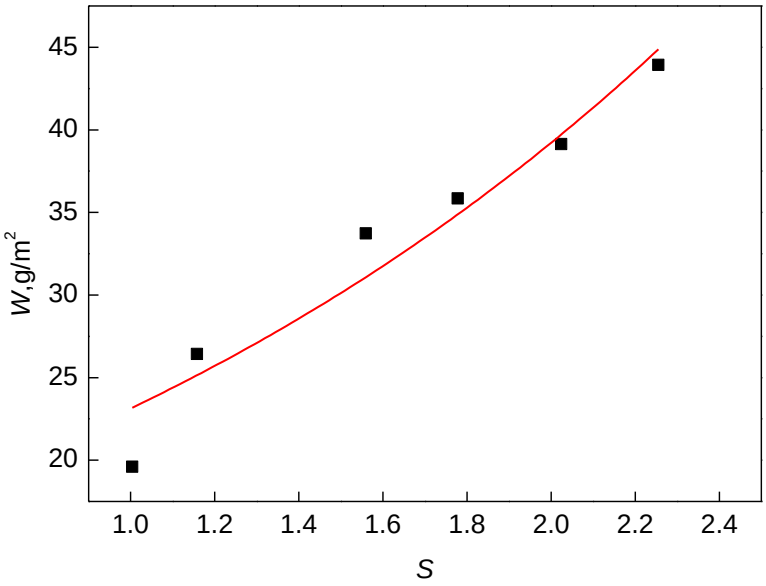

Figure 5. The relationship between feature value *S* and corrosion weight loss *W*

It can be found from Fig.5 that there was a direct relationship between the corrosion weight loss W and the feature value of S. Therefore, the feature value can be used to predict the corrosion weight loss and the precision is good. Compared with the weight change measurement,the wavelet packet decomposition–based image analysis method has the potential of allowing easier data acquisition, and may be a powerful method for the assessment of materials corrosion if combined with statistical analysis[13-15]. In addition, image analysis method based on WPD can overcome the problem that wavelet analysis only performing the decomposition process on approximations. In the paper,this method was proved to be an appropriate tool to analysis and quantify the corrosion damage from image of Q235 steel.

5. SUMMARY

In this paper, the corrosion 3D morphology image acquisition system that can be used in the field was established.

The image analysis method based on wavelet packet was used to study the corrosion morphology of Q235 steel specimens which exposed to the simulated atmospheric environment. Wavelet packet transformation was applied to decompose the denoise images. Energies of sub-images which were calculation according to Shannon entropy criterion were extracted as characteristic information.

The corrosion extent of Q235 steel specimens was qualitatively analyzed and it correlated well with the change of the energies of sub-images. Results showed that, the smaller energy value is, the slighter the sample corrodes could be. The relationship between the feature value S (sum of the energy of all selected sub-images) and corrosion weight loss W of samples was evaluated by regression analysis, results showed that, the relationship between W and S is W=13.64e0.527S (R=92.4%). By using the equation obtained from the regression analysis, the corrosion degree of Q235 steel specimens can be quantitatively analyzed. The proposed method can be used to predict the atmospheric corrosion of Q235 steel.

ACKNOWLEDGEMENT
The authors wish to thank the National Natural Science Foundation of China (No.51131007) and Natural Science Foundation of Tianjin (No. 10JCYBJC03200) for support during the writing of this paper.

References

1. M.Natesan, G. Venkatachari and N. Palaniswamy, *Corros. Sci.* 48 (11) (2006) 3584–3608.
2. A. Porro, T.F. Otero, A.S. Elola, *Br. Corr. J.* 27 (3) (1992) 231–235.
3. J.P. Cai, M. Liu, Z.H. Luo, Z.H. Tang, B. Li, X.Y. Zhang, F. Lu, C.H. Tao, *J. Chin. Soc. Corros. Prot.* 25 (5) (2005) 262–266 (in Chinese).
4. I.O. Wallinder, C. Leygraf, *Corros. Sci.* 43 (12) (2001) 1396–2379.
5. M. Natesan, G. Venkatachari, N. Palaniswamy, *Corros. Sci.* 48 (11) (2006)3584–3608.
6. D. H. Xia, S. Z. Song, J. H. Wang, H. C. Bi, Z. W. Han, *T. Nonferr. Metal Soc.*, (2012) 717-724
7. D. H. Xia, S. Z. Song, J. H. Wang, H. C. Bi, Z. W. Han, *ActaPhys-Chim. Sin.*, 28 (2012) 121-126.
8. D. H. Xia, S. Z. Song, J. H. Wang, J. B. Shi, H. C. Bi, Z. M. Gao, *Electrochem. Commun.*, 15 (2012) 88-92.
9. A.Y.M. Peng, S.B. Lyon, G.E. Thompson, J.B. Johnson, *Br. Corros. J.* 28(2) (1993) 103–106.
10. J.W.J. Silva, A.G. Bustamante, E.N. Codaro, R.Z. Nakazato, L.R.O. Hein, *Appl. Surf.Sci.* 236 (2004) 356.
11. E.N. Codaro, R.Z. Nakazato, A.L. Horovistiz, L.M.F. Ribeiro, R.B. Ribeiro, L.R.O. Hein, *Mater. Sci. Eng.* A 334 (2002) 298.
12. G.N. Frantziskonis, L.B. Simon, W. Jung, T.E. Matikas, *Eur. J. Mech. A: Solids* 19(2000) 309.
13. L.Tao, S.Z.Song, S.Y. Wang, X.Y. Zhang, M.Liu, F.Lu, *Mater. Sci. Eng.*, A476(2008)210-216.
14. L.Tao, S.Z.Song, X.Y. Zhang, Z.Zhang, F.Lu, *Appl. Surf. Sci.*, 254(2008) 6870-6874.
15. S.Y. Wang, S.Z.Song, *Mater. Sci. Eng.* , A385(2004)377-381.
16. D. H. Xia, S. Z. Song, W. Q. Gong, Y. X. Jiang, Z. M. Gao, *J. H. Wang, J.Food Eng.*, 113 (2012) 11-18.
17. D. H. Xia, S. Z. Song, J. H. Wang, H. C. Bi, *CIESC Journal*, 63 (2012) 1797-1802.
18. D. H. Xia, S. Z. Song, J. H. Wang, H. C. Bi, Z. W. Han, *Trans. Tianjin Univ.*, 18 (2012) 15-20.
19. K.Daqrouq, *Eng. Appl. Artif. Intell.*, 24(2011)796-802.

20. D.Wang, D.Q.Miao, C.Xie, *Expert Systems with Applications*. 38(2011)14314-14320
21. X.Y.Luo, F.L. Liu, D.S.Wang, *Journal of communication*， 29(10)(2008)173-182(in Chinese).
22. J.D.Wu, B.F.Lin, *Expert Systems with Applications*, 36(2009)3136–363143.
23. Z.X. Cheng. Wavelet analysis algorithm and application. Xi'an: *Xi 'an Jiaotong University Press*, 2004:156(in Chinese).
24. Y.K.Sun. Wavelet Analysis and Application. Beijing: *China Machine Press*, 2005：160(in Chinese).
25. Livens S. PhD Dissertation, Antwerpen University, Antwerp, Belgium, 1997.
26. C.H.Dong. Matlab wavelet analysis toolbox principle and application. Beijing: *National Defense Industry Press*, 2004:30(in Chinese).